IRAQI JOURNAL OF APPLIED PHYSICS
Vol. 22, No. 2, April-June 2026, pp. 205-212

Simulation of CBTS Thin-Film Solar Cells: Effect of Surface Defects and Layer Thickness Using SCAPS-1D

Ali H. Mohammed [1*]
Shahed A. Dheyab [2]
Muatazbullah I. Abdullah[3]

[1,2] Department of Physics, College of Education for Pure Sciences, Tikrit University, Tikrit, IRAQ
[3] Ministry of Education Directorate General of Education in Kirkuk, Al-Jawhara Intermediate School for Girls, Kirkuk, IRAQ
* Corresponding author email: ali.hu.mohammed@tu.edu.iq

The simulation results indicate that surface defects at the CdS/CBTS interface strongly degrade the performance of CBTS solar cells. Increasing defect density reduces the fill factor (FF) from ~25.8% to 25.1%, reflecting the limited ability of the device to maintain high current at optimal voltage due to enhanced recombination. Efficiency (η) decreases from ~0.7% to 0.22%, driven by reductions in open-circuit voltage (V_{oc}) and short-circuit current density (J_{sc}). Specifically, V_{oc} drops from ~0.65 V to 0.37 V, while J_{sc} decreases from ~4.2 mA/cm^2 to 2.5 mA/cm^2 at the highest defect levels. These changes are attributed to increased recombination centers and shortened carrier lifetimes, which hinder charge transport to the electrodes. Overall, the results confirm that minimizing interfacial defect density is critical to improving photovoltaic performance. Enhancing interfacial quality and suppressing recombination are therefore essential strategies for achieving higher efficiency in CBTS thin-film solar cells.

Keyword: Thin film solar cells; Surface defects; SCAPS-1D; Quantum efficiency
Received: 10 July 2025; Revised: 10 September; Accepted: 17 September 2025

1. Introduction

The ever-increasing global demand for energy, coupled with the rapid depletion of fossil fuel resources and the environmental challenges associated with greenhouse gas emissions, has accelerated the search for sustainable and renewable energy alternatives. Among these, solar photovoltaics have emerged as one of the most promising solutions due to their clean, abundant, and inexhaustible nature. In particular, thin-film solar cells have attracted remarkable attention because of their low material consumption, cost-effectiveness, and potential for large-scale production [1-6].

Over the past decades, chalcogenide-based thin-film absorbers such as Cu(In,Ga)Se_2 (CIGS) and CdTe have achieved impressive power conversion efficiencies exceeding 20%. However, the scarcity and toxicity of their constituent elements (In, Ga, Cd, and Te) impose serious limitations for large-scale deployment. This has stimulated intensive research into alternative earth-abundant, non-toxic, and cost-effective materials. One promising candidate is copper barium tin sulfide (CBTS), a quaternary chalcogenide semiconductor with a direct bandgap of ~1.9 eV and a high absorption coefficient (>10^5 cm^{-1}). Its non-toxic nature and abundance of constituent elements make CBTS a sustainable alternative for next-generation thin-film photovoltaics [7-13].

Despite these advantages, the efficiency of CBTS-based solar cells remains relatively low, typically below 5%, mainly due to non-radiative recombination processes associated with surface and interface defects, as well as limitations related to layer thickness optimization. Surface defects act as recombination centers, reducing carrier lifetime and deteriorating device performance, while improper buffer and absorber thicknesses limit light absorption and carrier transport. Therefore, addressing these issues is essential for unlocking the full potential of CBTS thin-film solar cells [14].

Numerical simulation has become a powerful tool to explore these limitations, providing a cost-effective and predictive means to study device physics and optimize structural parameters. The SCAPS-1D (Solar Cell Capacitance Simulator) software, developed at Ghent University, has been widely used to model a variety of thin-film solar cells, offering insights into the effects of defects, doping, and layer thicknesses on photovoltaic performance [15].

In this work, SCAPS-1D is employed to systematically investigate the influence of surface defect density and layer thickness (CdS buffer and CBTS absorber) on the performance of ITO/ZnO/CdS/CBTS thin-film solar cells. The aim is to identify the optimal structural parameters that minimize recombination losses and maximize efficiency, thereby providing a pathway toward improving the competitiveness of CBTS as a sustainable absorber material for thin-film photovoltaics.

2. SCAPS Numerical Simulation

The University of Ghent in Belgium created SCAPS, a one-dimensional solar cell modeling program, to mimic both conventional semiconductor crystalline materials like CIGS and CdTe and non-traditional materials like SnS. To specify properties like optical absorbance, thickness, doping concentration, energy gap, and more, the user can create a cell with as many as seven layers. It is possible to determine spectral responses in both dark and light environments by varying the temperature. Everything related to solar cells has been incorporated into this program. It is a freely available program [16]. Which works by solving the semiconductor equations we start by writing Boswin's equation [17]:

$$\nabla(E) = \frac{q}{\varepsilon}(p - n + N_D^+ - N_A^-) \quad (1)$$

The equation uses the following variables: E, q, the absorber's permittivity, n(p), the density of electrons (holes), and N_D (N_A), the concentration of donors (acceptors). As a result, the following link offers the continuity equation [18]:

$$\frac{dn}{dt} = \frac{1}{q}(\nabla (J_n) + G_n - R_n \quad (2)$$

$$\frac{dp}{dt} = - \frac{1}{q}(\nabla \left(J_p \right) + G_p - R_p \quad (3)$$

where J_n (J_p) is the current density of electrons (holes), G_n (G_p) is the generation rate of electrons (holes), and Rn (R_p) is the recombination rate of electrons (holes)

The charge carrier equations for diffusion and drift current densities may be obtained using the following formulae [19]:

$$J_n = q(\mu_n nE + D_n \nabla n) \quad (4)$$

$$J_p = q\left(\mu_p PE + D_p \nabla p \right) \quad (5)$$

where n (p) is the electron (hole) mobility and D is the diffusion constant. The filling factor (FF), short circuit current (J_{sc}), open circuit voltage (V_{oc}), and conversion efficiency must all be understood in order to determine the quality of photovoltaic cells, as these variables are linked by the following equations [20]

$$FF = \frac{P_{max}}{P_t} \frac{V_{max} . I_{max}}{Voc . J_{sc}} \quad (6)$$

$$\eta = \frac{P_m}{P_{in}} = \frac{Voc.Jsc. FF}{P_{in}} \quad (7)$$

where V_{max} is the maximum voltage, P_{max} is the maximum power, I_{max} is the maximum current, and P_{in} is the incoming power

The following relationship between doping concentration and recombination and minority carrier age, which is the average length of time required for their recombination, may be utilized to determine minority carrier age [21]

$$\tau = \frac{1}{\sigma V_{th} N_t} \quad (8)$$

$$\boldsymbol{\tau} = \frac{\Delta n}{U} \quad (9)$$

The concentration of defects, denoted as N_t, is related to the thermal speed, conductivity, recombination rate, and excess minority carrier concentration, denoted as V_{th}

3. Structure of Solar Cells

The constituent parts of an ITO/ZnO/CdS/CBTS solar cell are an ITO/ZnO window layer, which consists of transparent metal oxides and has a larger energy gap than the subsequent layers. The CdS buffer layer has an energy gap that is appropriate for the absorption layer gradient with transmission, and the CBTS absorption layer has an energy gap as well. Very small, with a work function of 5 eV, a glass floor beneath the cell, and front and back contacts made of gold [22]. Table (1) displays the SCAPS software parameters that need to be entered to examine the experimental cell's performance, along with the values of the defects between the absorption layer and the transmittance. Temperature was 300 K, resistance was 85 Ω in parallel and 69.5 Ω in series.

Table (1) The physical parameters of different layers

Parameters	CBTS	Cds	Zno	ITO
Thickness	0.23	0.05	0.05	0.16
Bandgap	1.94	2.4	3.3	3.6
Electron affinity	3.6	4.2	4.4	4.1
Dielectric permittivity	5.4	10	9	10
CB effective density of States	2.2E+18	2.2E+18	2.2E+18	2E+18
VB effective density of States	1.8E+19	1.8E+19	1.8E+19	1E+19
Electron thermal velocity	30	100	100	75
Hole thermal velocity	10	25	25	50
Shallow uniform donor Density	0	1E+16	1E+16	1E+19
Shallow uniform acceptor Density	1E+13	0	0	0
Coefficient absorption	5E+4	SCAPS	SCAPS	1E+5

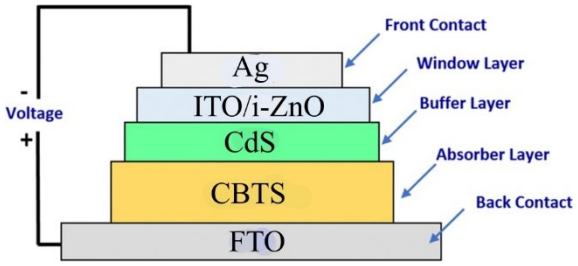

Fig. (1) The structure of the CBTS cell

4. Results and Discussion

Figure (2) shows the simulation results of surface defect effects on the performance of the CBTS solar cell reveal that all photovoltaic parameters are adversely influenced by increasing defect density at the CdS/CBTS interface. The fill factor (FF) decreases noticeably from approximately 25.8% at the lowest defect density to about 25.1% at higher values, reflecting the reduced capability of the cell to sustain a high current at the optimum voltage due to the rise in recombination centers. Similarly, the overall efficiency (η) follows the same trend, dropping from around 0.7% to 0.22% as the surface defect density increases. This decline can be attributed to reductions in both the open-circuit voltage (V_{oc}) and the short-circuit current density (J_{sc}). Specifically, V_{oc} decreases from ~0.65 V to ~0.37 V, while J_{sc} decreases from ~4.2 mA/cm² to

~2.5 mA/cm² at the highest defect density. Such performance degradation is caused by enhanced recombination rates of photogenerated carriers and the shortened carrier lifetime, which limit their ability to reach the electrodes [23]. Therefore, improving the interfacial quality and minimizing the surface defect density are crucial factors for enhancing the efficiency of thin-film CBTS solar cells.

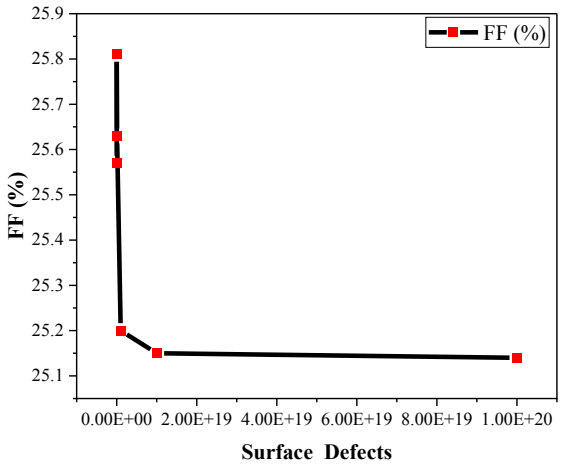

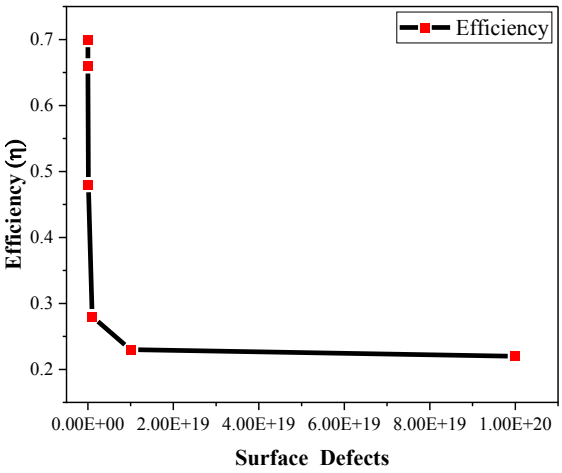

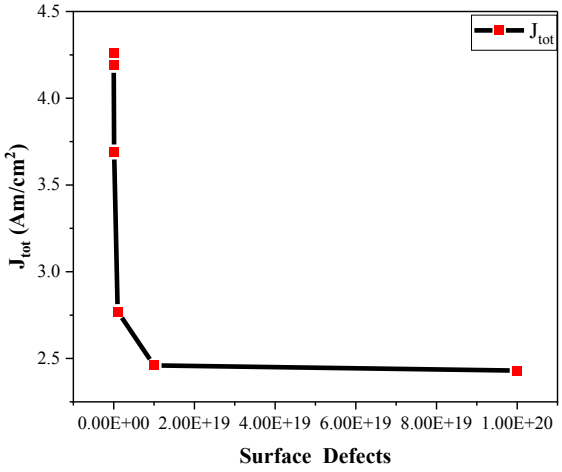

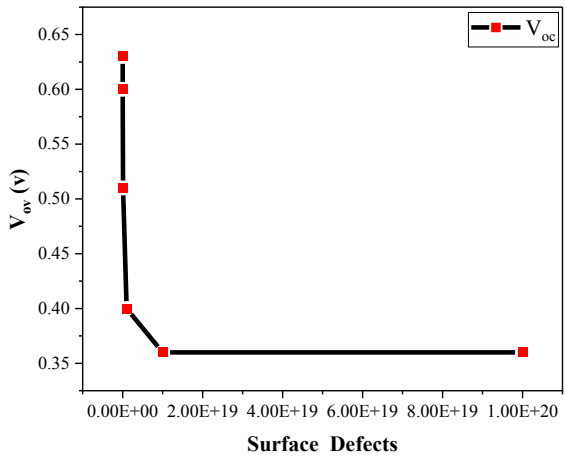

Fig. (2) The surface defects as a function of cell output

Figure (3) shows the quantum efficiency (QE) spectrum of the CBTS solar cell as a function of wavelength and demonstrates the device's spectral response across the visible region. The QE increases gradually from ~5% at 100 nm to about 20% near 400 nm, indicating effective absorption of high-energy photons. A pronounced enhancement is observed between 450–550 nm, where QE reaches its maximum value of approximately 43% at ~520 nm, reflecting the optimal absorption characteristics of the CBTS absorber layer within this spectral range. Beyond 550 nm, the QE declines sharply, approaching nearly zero at ~700 nm, which corresponds to the absorption edge of the CBTS material and is consistent with its bandgap energy (~1.9 eV). This behavior confirms that the CBTS absorber layer exhibits strong photo-response within the visible range, while its performance diminishes significantly in the near-infrared region due to limited photon absorption [24]. The results emphasize that improving the absorber quality and minimizing recombination losses could further enhance the device's spectral response and overall efficiency.

Figure (4) shows the current density–voltage (J–V) characteristics of the CBTS solar cell under different surface defect densities. It is evident that as the defect density increases from 1×10^{15} cm^{-3} to 1×10^{20} cm^{-3}, both the forward and reverse bias current densities deteriorate. At low defect density (1×10^{15} cm^{-3}), the device exhibits higher current density values, with improved slope in the forward bias region, indicating enhanced carrier collection and reduced recombination losses. However, with the progressive increase of defect density, the current density decreases significantly, and the J–V curves shift downward, reflecting stronger recombination at the CdS/CBTS interface and a reduced ability of the cell to generate photocurrent [25]. This behavior highlights the detrimental role of surface defects on charge carrier transport and confirms that minimizing defect density is essential for improving both the open-circuit voltage

and short-circuit current, thereby enhancing the overall device efficiency.

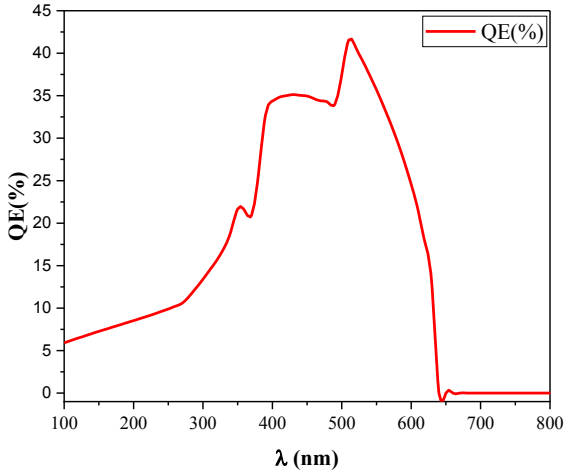

Fig. (3) The relationship between wavelength and quantum efficiency

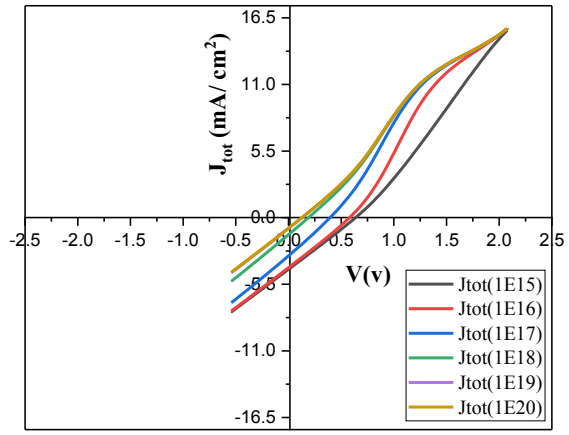

Fig. (4) The relationship between voltage and current for different surface defects

Figure (5) shows the spectral response of the CBTS solar cell expressed as quantum efficiency (QE%) for different surface defect densities ranging from 1×10^{15} cm^{-3} to 1×10^{20} cm^{-3}. At the lowest defect density (1×10^{15} cm^{-3}), the device exhibits the highest QE, reaching nearly 95% at ~500 nm, with strong response across the visible spectrum. As the defect density increases, the QE decreases markedly at 1×10^{17} cm^{-3}, the peak QE drops to around 70%, while at higher defect levels (1×10^{19}-1×10^{20} cm^{-3}) the spectral response is severely suppressed, with QE values below 40% and negligible response beyond 600 nm. This degradation is attributed to the enhanced recombination of photogenerated carriers at the CdS/CBTS interface and within the absorber bulk, which reduces the carrier collection efficiency [26]. The results confirm that minimizing surface defects is critical to maintaining strong photoresponse and achieving high spectral efficiency in CBTS thin-film solar cells.

Figure (6) shows the influence of the CdS buffer layer thickness on the photovoltaic parameters of the CBTS solar cell. The fill factor (FF) increases with thickness, reaching a maximum of ~27.2% at ~2 nm before slightly declining at higher thicknesses. This trend indicates that a moderately thick CdS layer enhances interface quality and reduces recombination, while excessive thickness increases resistive losses, leading to reduced FF.

The short-circuit current density (J_{sc}) exhibits a similar trend, rising from ~4.2 mA/cm² at 0.25 nm to a maximum of ~5.5 mA/cm² at ~2 nm, before decreasing as the thickness approaches 5 nm. This behavior reflects the balance between improved photon transmission to the absorber at optimized thickness and increased absorption/blocking effects by the CdS layer when it becomes too thick.

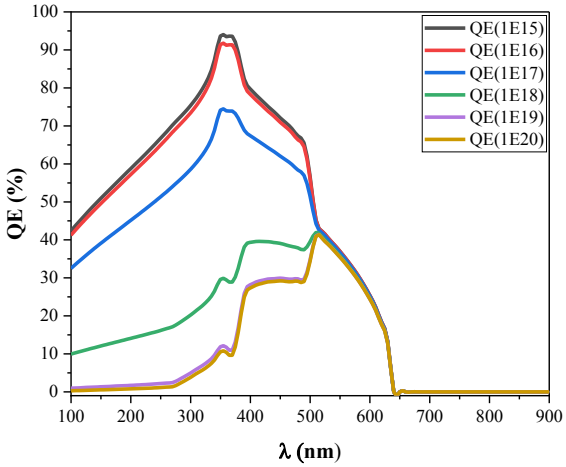

Fig. (5) The relationship between wavelength and quantum efficiency for different surface defects

The open-circuit voltage (V_{oc}) improves from ~0.62 V at 0.25 nm to ~0.74 V at ~2 nm, remaining nearly stable afterward, but slightly decreasing at excessive thickness due to recombination at the CdS/CBTS interface. Most importantly, the overall efficiency (η) rises significantly with increasing CdS thickness, from ~0.7% at 0.25 nm to a maximum of ~1.2% at ~2 nm, before gradually dropping at higher thickness values. This indicates that the optimal CdS buffer thickness lies around 2 nm, where the trade-off between reduced interface defects and minimal absorption losses is achieved, resulting in improved carrier transport and higher efficiency [27].

Figure (7) shows the quantum efficiency (QE) spectra of the CBTS solar cell at different absorber thicknesses. At very thin absorber layers (0.25–0.5 nm), the QE is relatively low across the visible range, with a maximum of ~70%, indicating limited photon absorption due to insufficient thickness. As the absorber thickness increases, the QE significantly improves, reaching values above 95% across 400–600 nm for thicknesses between 1.0 and 2.0 nm, reflecting

enhanced light absorption and efficient charge carrier generation.

Beyond 2.0 nm, the QE remains high but shows slight suppression at longer wavelengths (>600 nm), which may be attributed to increased recombination within the deeper regions of the absorber and reduced carrier collection efficiency. The optimal spectral response is observed at thicknesses of 1.5–2.0 nm, where the QE approaches unity in the visible region, confirming efficient photon-to-electron conversion.

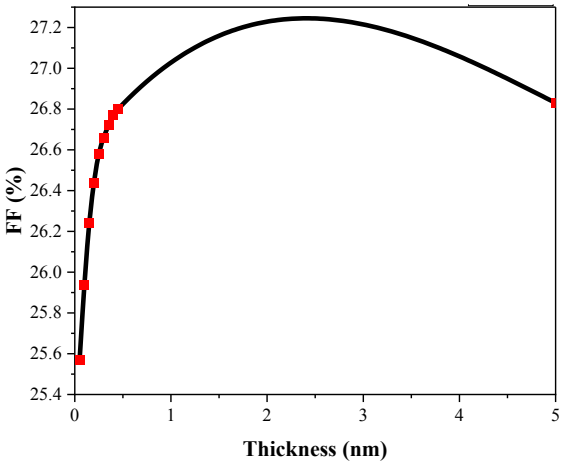

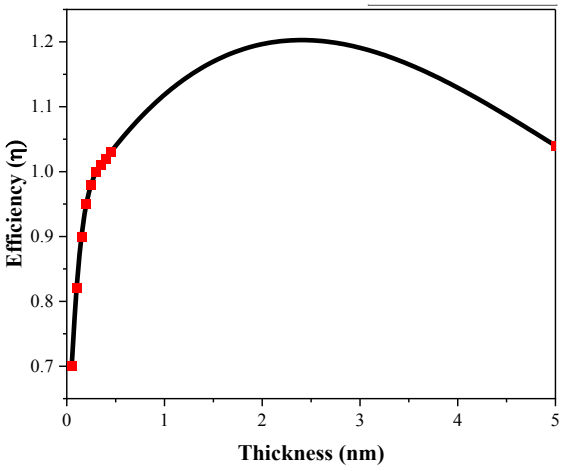

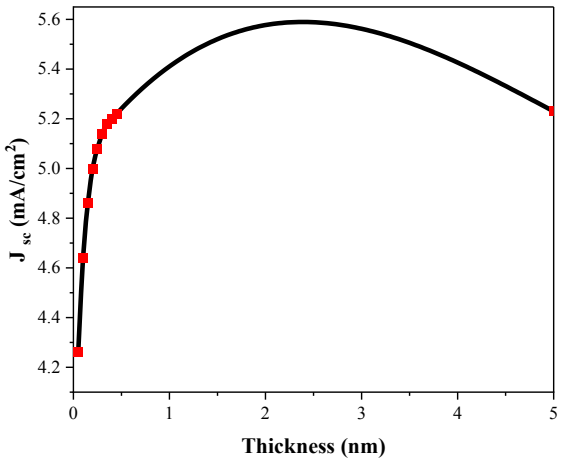

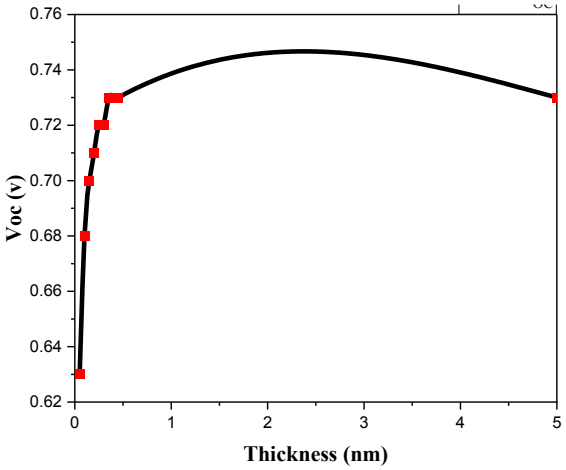

Fig. (6) The thickness as a function of cell output

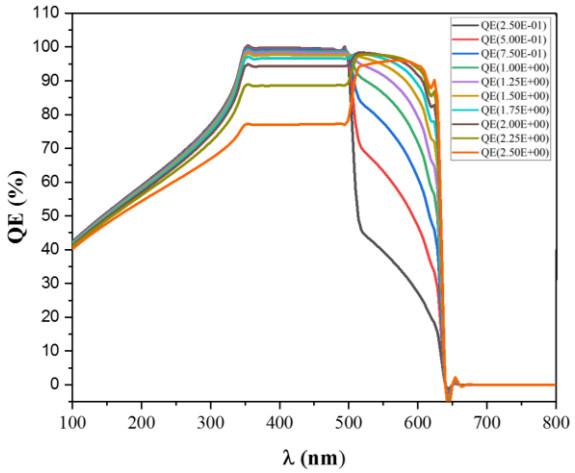

Fig. (7) The relationship between wavelength and quantum efficiency for different buffer thicknesses layer

These results highlight the critical role of absorber thickness in determining the spectral response of CBTS solar cells, where too thin layers fail to absorb sufficient photons, while excessively thick layers introduce recombination losses [28]. An optimized thickness ensures maximal QE and contributes to higher overall device efficiency.

Figure (8) shows the current density–voltage (J–V) characteristics of the CBTS solar cell for different CdS buffer layer thicknesses (ranging from 50 nm to 500 nm). It is evident that increasing the CdS thickness leads to improved current density under forward bias, particularly up to ~300 nm, beyond which the improvement becomes marginal. At thinner CdS layers (50-100 nm), the device suffers from reduced interface quality and higher recombination rates at the CdS/CBTS junction, resulting in lower photocurrent. As the thickness increases to an optimal range (200-300 nm), the J–V curve shifts upward, reflecting enhanced carrier collection and reduced recombination at the heterojunction interface. However, further increasing the CdS thickness beyond 300 nm results in negligible gains and even slight deterioration in current density, as

thicker CdS layers begin to absorb incident photons and hinder their transmission to the CBTS absorber [29]. This trade-off confirms that an optimized CdS buffer thickness (~250-300 nm) is crucial to achieving the best balance between interface passivation and optical transmission, thereby enhancing the photovoltaic performance of the CBTS solar cell.

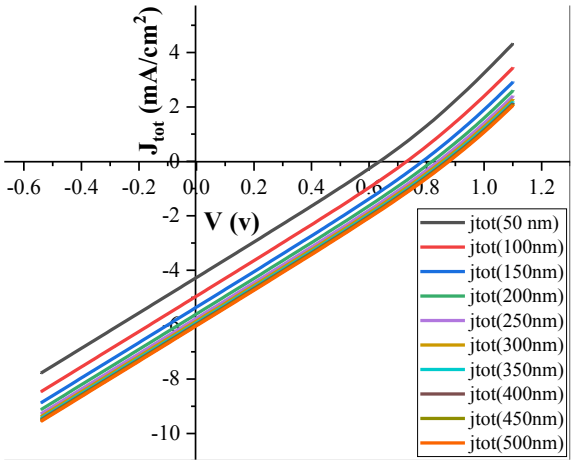

Fig. (8) Relationship between voltage and current for different buffer thicknesses layer

Figure (9) shows the effect of absorber thickness on the photovoltaic performance of the CBTS solar cell. As shown in these figures, the fill factor (FF) initially increases with thickness, reaching its maximum (~29.2%) at around 0.75 nm, before gradually declining at higher thicknesses, which is likely attributed to increased series resistance and reduced carrier collection efficiency. The short-circuit current density (J_{sc}), on the other hand, exhibits a continuous rise with thickness, increasing from ~5.2 mA/cm² at 0.25 nm to ~7.9 mA/cm² at 2.25 nm. This trend reflects the enhanced photon absorption and generation of charge carriers as the absorber becomes thicker.

The open-circuit voltage (V_{oc}) remains relatively stable across most thickness values (~0.76 V), showing only minor fluctuations, with a slight reduction observed at the maximum thickness, which could be due to recombination losses at deeper regions of the absorber layer [30]. Most importantly, the overall conversion efficiency (η) improves significantly with increasing absorber thickness, rising from ~1.0% at 0.25 nm to a peak of ~1.7% at 1.75 nm, after which it slightly decreases. This indicates that an optimal thickness exists, beyond which recombination effects outweigh the benefits of enhanced absorption.

These findings highlight that while increasing the CBTS absorber thickness improves light harvesting and photocurrent generation, excessive thickness leads to efficiency losses due to recombination and resistive effects. The optimal thickness in this study is around 1.75-2.0 nm, where the balance between absorption and carrier collection is best achieved, resulting in maximum device efficiency.

Table (2) The theoretical and experimental results of the ITO/ZnO/CdS/CBTS solar cell

S	Cells	V(V)	J(mA/cm²)	FF	η(%)
1	Experimental	0.37	2.56	29	0.27
2	Theoretical	0.371	2.56	25.2	0.26

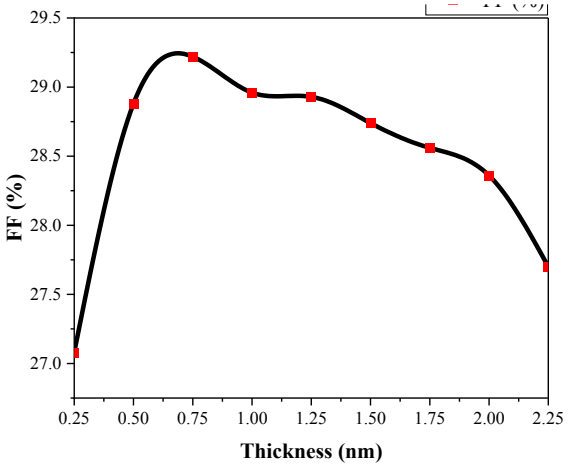

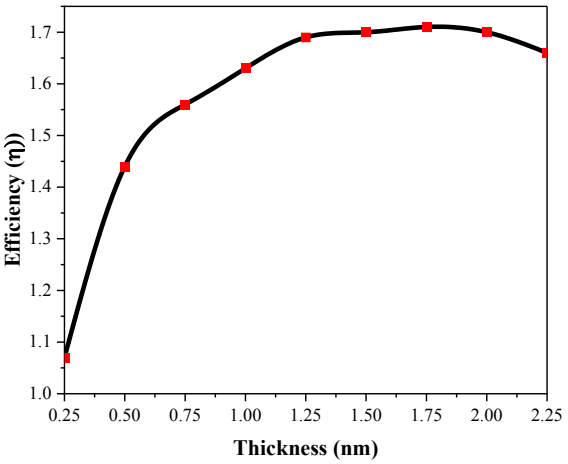

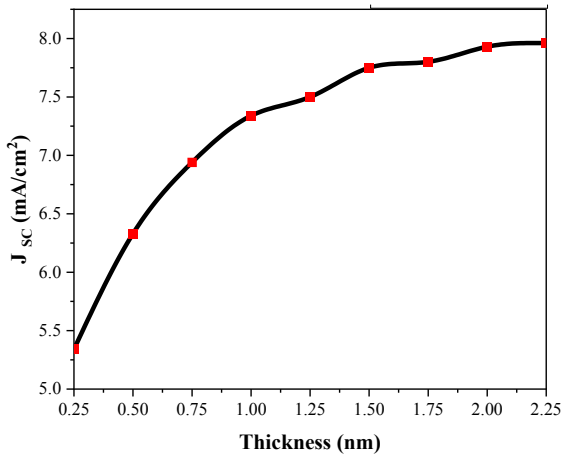

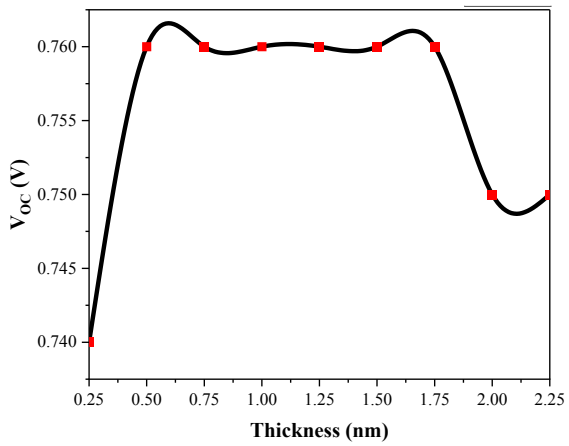

Fig. (9) The solar cell parameters as functions of thickness of the absorbing layer

5. Conclusions

The SCAPS-1D simulation demonstrated that surface defect density critically affects CBTS solar cell performance. Reducing defects at the CdS/CBTS interface from 1×10^{20} to 1×10^{15} cm^{-3} increased efficiency to 0.70%, V_{oc} to 0.65 V, J_{sc} 4.2 mA/cm², and FF to 25.8%. Quantum efficiency also peaked at ~95% around 520-550nm at the lowest defect density, confirming the role of passivation. Optimizing CdS buffer thickness (50-300nm) further enhanced performance, achieving 1.2% efficiency, J_{sc} ~5.5 mA/cm², and V_{oc} ~0.74 V, while thicker layers (>400nm) introduced parasitic absorption and reduced output. Similarly, absorber thickness (0.25-2.0µm) strongly influenced performance as the efficiency increased to 1.7%, J_{sc} to 7.9 mA/cm², and FF peaking at ~29.2% before declining due to recombination. QE exceeded 95% across 400-600nm at 1.5-2.0 µm thickness. Overall, simultaneous optimization of surface defects, buffer, and absorber thickness boosted efficiency from 0.26% to 1.7%, highlighting the key role of defect passivation and thickness engineering in CBTS devices.

References

[1] Z.I. Subašić, F. Sher and E. Papraćanin, "Solar photovoltaic energy technologies", Ch. 7, F. Sher (ed.), **Renewable Energy Technologies**, Elsevier (2026), pp. 219-274.

[2] H. Luo et al., "Controlled synthesis of high efficiency Cu_2BaSnS_4 solar cells via a solution processed method", *Mater. Lett.*, 270 (2020) 127750.

[3] R. Chakraborty and P. Ghosh, "Mechanistic insights of hydrogen evolution reaction on quaternary earth-abundant chalcogenide Cu_2BaSnS_4 from first principles", *Appl. Surf. Sci.*, 570 (2021) 151049

[4] A. Ali et al., "Cu_2BaSnS_4 novel quaternary quantum dots for enhanced photocatalytic applications", *Mater. Today Commun.*, 26 (2021) 101675.

[5] M. Suresh Kumar, S.P. Madhusudanan and S.K. Batabyal, "Solution-processed photoactive trigonal Cu_2BaSnS_4 thin films for efficient solar energy harvesting", *Mater. Characteriz.*, 174 (2021) 110988.

[6] E. Djatoubai and J. Su, "First spray pyrolysis thin film fabrication of environment-friendly Cu_2BaSnS_4 (CBTS) nanomaterials", *Chem. Phys. Lett.*, 770 (2021) 138406.

[7][2] D.R. Sajitha et al. "The emergence of chalcogenides: A new era for thin film solar absorbers", *Prog. Solid State Chem.*, 76 (2024) 100490.

[8][3] V. Karade et al. "Opportunities and Challenges for Emerging Inorganic Chalcogenide-Silicon Tandem Solar Cells", *Energy Environ. Sci.*, 18 (2025) 6899-6933.

[9] A. Sharma et al., "Visible-light induced photosplitting of water using solution-processed Cu_2BaSnS_4 photoelectrodes and a tandem approach for development of Pt-free photoelectrochemical cell", *Mater. Sci. Semicond. Process.*, 121 (2021) 105433.

[10] B.C.M. Jyoti, "Barium concentration controlled phase evolution in molecular solution processing of Cu_2BaSnS_4 thin films for solar cells with improved optical and electrical properties", *J. Alloys Comp.*, 986 (2024) 174105.

[11] A.S. Kadari et al., "Growth and optimization of spray coated Cu_2BaSnS_4 thin films for solar photovoltaic application", *Materialia*, 36 (2024) 102178.

[12] M.T. Alemu et al., "Computational investigation of Sb-doping of $CsSnI_3$: Insights into structural, electronic, optical, and photovoltaic performance analysis", *Computat. Mater. Scie.*, 258 (2025) 114060.

[13] A. Chihi, "Effect of cobalt doping on the physicochemical and photocatalytic properties of Cu_2BaSnS_4 thin films", *RSC Adv.*, 15(42) (2025) 35660-35676.

[14] S.M. Sivasankar, C.d.O. Amorim and A.F. da Cunha, "Progress in thin-film photovoltaics: A review of key strategies to enhance the efficiency of CIGS, CdTe, and CZTSSe solar cells", *J. Compos. Sci.,* 9(3) (2025) 143.

[15] Md.D. Haque et al., "Numerical analysis for the efficiency enhancement of MoS_2 solar cell: a simulation approach by SCAPS-1D", *Opt. Mater.,* 131 (2022) 112678.

[16] F. Baig, "Numerical analysis for efficiency enhancement of thin film solar cells", Dissertation, Universitat Politècnica de València (2019).

[17] O. Skhouni et al., "Numerical study of the influence of ZnTe thickness on CdS/ZnTe solar cell performance", *The Euro. Phys. J. Appl. Phys.,* 74(2) (2016) 24602.
[18] K.Y. Hameed et al., "Modelling of novel-structured copper barium tin sulphide thin film solar cells", *Bull. Mater. Sci.,* 42(5) (2019) 231.
[19] R. Ganvir, "Modelling of the nanowire CdS-CdTe device design for enhanced quantum efficiency in Window-absorber type solar cells", MSc thesis, University of Kentucky (2016).
[20] A. Rothwarf and K.W. Böer, "Direct conversion of solar energy through photovoltaic cells", *Prog. Solid State Chem.,* 10 (1975) 71-102.
[21] F. Elmourabit, Y. Essakali and S. Dlimi, "Numerical investigation of CdS/CdTe thin-film solar cells using SCAPS-1D: Influence of layer thickness and temperature on device performance", *Hybrid Adv.*, 12 (2026) 100582.
[22] H. Guo et al., "The fabrication of Cu_2BaSnS_4 thin film solar cells utilizing a maskant layer", *Solar Energy*, 181 (2019) 301-307.
[23] Z. Song et al., "Perovskite solar cells go bifacial—mutual benefits for efficiency and durability", *Adv. Mater.,* 34(4) (2022) 2106805.
[24] M. Salem et al., "Optimizing transport carrier free all-polymer solar cells for indoor applications: TCAD simulation under White LED illumination", *Polymers,* 16(10) (2024) 1412.
[25] B. Teymur, "Solution-Processed Thin Film Deposition and Characterization of Multinary Chalcogenides: Towards Highly Efficient $Cu_2BaSn(S,Se)_4$ Solar Devices", Dissertation, Duke University (2022).
[26] T.A. Chowdhury, "SCAPS numerical modeling of CBTS/WO_3 thin film solar cell", *Optics Continuum*, 3(11) (2024) 2190-2217.
[27] J. Dong et al., "Carrier management through electrode and electron-selective layer engineering for 10.70% efficiency antimony selenosulfide solar cells", *Nature Energy*, 10 (2025) 857-868.
[28] S.M.H. Qaid et al., "Optimizing CBTSSe solar cells for indoor applications through numerical simulation", *Opt. Quantum Electron.,* 55(14) (2023) 1245.
[29] G. Siddharth et al., "Progress in Thin Film Solar Cell and Advanced Technologies for Performance Improvement", A.-G. Olabi (ed.), **Encyclopedia of Smart Materials**, Elsevier (2022), pp. 661-680.
[30] X. Hu et al., "Improving the efficiency of Sb_2Se_3 thin-film solar cells by post annealing treatment in vacuum condition", *Sol. Ener. Mater. Solar Cells,* 187 (2018) 170-175.

